ELSEVIER

Physica C 282–287 (1997) 323–326

PHYSICA C

Vortex Matter Phase Transitions in $Bi_2Sr_2CaCu_2O_8$

R. A. Doyle[a,b], B. Khaykovich[a,c], M. Konczykowski[c], E. Zeldov[a], N. Morozov[a,c], D. Majer[a], P. H. Kes[d], and V. Vinokur[e]

[a]Department of Condensed Matter Physics, The Weizmann Institute of Science, 76100 Rehovot, Israel
[b]IRC in Superconductivity, University of Cambridge, Cambridge CB3 0HE, United Kingdom
[c]CNRS, URA 1380, Laboratoire des Solides Irradiés, École Polytechnique, 91128 Palaiseau, France
[d]Rijksuniversiteit Leiden, P. O. Box 9506, 2300 RA Leiden, The Netherlands
[e]Materials Science Division, Argonne National Laboratory, Argonne, Illinois 60439

Vortex-lattice phase transitions in $Bi_2Sr_2CaCu_2O_8$ crystals are studied using local magnetization measurements. The vortex matter is found to exhibit at least three distinct phases. A rather ordered quasilattice phase is present at low fields. At elevated temperatures the quasilattice melts (or sublimates) through a first-order phase transition, whereas at lower temperatures a transition to a highly disordered vortex solid occurs at the second magnetization peak. A very low density of columnar defects results in significant pinning of the quasilattice, demonstrating the finite shear modulus of this phase. Local ac measurements reveal that in the presence of columns the pinned quasilattice still melts through a first-order phase transition with an observable step in equilibrium magnetization at elevated temperatures.

1. INTRODUCTION

The high-temperature superconductors (HTSC) in the mixed state display a very complicated phase diagram. The nature of the different vortex phases and the transitions between them are still unclear. In the low temperature superconductors it was believed that only one thermodynamic phase, a solid Abrikosov lattice, exists in the mixed state. Since the discovery of HTSC it has became apparent that thermal fluctuations play a crucial role and may result in melting of the lattice, thus forming two phases, vortex solid and vortex liquid. However in highly anisotropic HTSC like $Bi_2Sr_2CaCu_2O_8$ (BSCCO) the vortex matter phase diagram is much more complicated and displays at least three distinct phases as shown in Fig. 1. We have incorporated a very low dose of columnar defects in order to elucidate the structure of the various phases. We find that low concentrations of columnar defects have an observable effect only in the low field quasilattice phase, resulting in significantly enhanced pinning in this state. The pinned quasilattice still displays a first-order melting transition at elevated temperatures.

2. EXPERIMENTAL

The experiments were carried out on several BSCCO crystals [1] with typical dimensions of $700 \times 300 \times 10\ \mu m^3$. The crystals were irradiated by 1 GeV Xe or 0.9 GeV Pb ions at GANIL (Caen, France), which produced uniform columnar defects parallel to the crystalline c-axis. We have investigated very low irradiation doses corresponding to matching fields B_ϕ in the range of 20 to 100 G ($B_\phi = n\phi_0$, where n is the density of the columnar tracks and ϕ_0 is the magnetic flux quantum). The local magnetization measurements were performed in applied field $H_a||z||c$-axis using arrays of $10 \times 10\mu m^2$ GaAs/AlGaAs Hall sensors [2]. The sensors measure the perpendicular component of the local induction B_z at various locations across the sample. For ac studies a small ac field H_{ac} was superimposed onto the dc magnetic field H_{dc} and the resulting local ac induction B_{ac} across the crystal was measured using lock-in techniques.

3. PHASE TRANSITIONS

Figure 1 shows the phase diagram of the vortex matter in BSCCO as inferred from our local

PII S0921-4534(97)00277-3

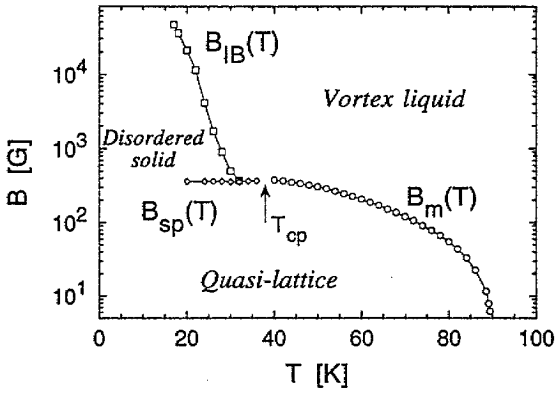

Figure 1: Vortex matter phase diagram in BSCCO displaying three distinct phases with three boundary lines. The quasilattice phase melts through a FOT at $B_m(T)$ and transforms into a disordered solid through a disorder-induced transition at B_{sp}. The disordered solid melts continuously along $B_{IB}(T)$.

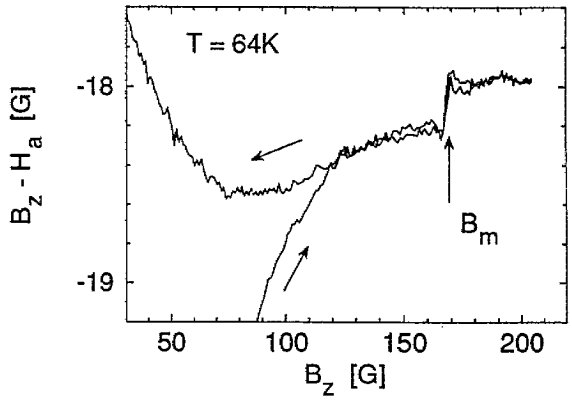

Figure 2: Local magnetization loop at elevated temperature showing the FOT manifested by the sharp step in equilibrium magnetization at $B_m(T)$.

magnetization measurements. There are three experimentally observed phase boundary lines. At elevated temperatures and low fields a first-order phase transition (FOT) is observed. Local magnetization measurements $B_z - H_a$ vs. B_z display a small positive sharp step in equilibrium magnetization at the transition as shown in Fig. 2. A similar step is observed by temperature scans [2]. The position of the FOT line $B_m(T)$ is shown in Fig. 1. The FOT line terminates abruptly at intermediate temperatures at a critical point T_{cp} as indicated by the arrow in Fig. 1.

At temperatures below the critical point an onset of a large second magnetization peak [3] is observed at $B_{sp}(T)$ as shown in Fig. 3. Analysis of the field profiles across the sample shows a transition from smooth dome-shaped profiles due to surface and geometrical barriers at low fields to Bean profiles due to the onset of significant critical currents at fields above B_{sp} [4]. Local magnetization measurements indicate that this transition is very sharp [5]. We therefore infer that the sharp change in the apparent pinning at the onset of the second peak is driven by an underlying thermodynamic phase transition.

It is interesting to note that the second peak line $B_{sp}(T)$ and the FOT line $B_m(T)$ meet at the critical point forming one continuous transition line. Similar investigations were carried out on oxygen annealed crystals with various anisotropy [5,6]. The position of $B_{sp}(T)$ and $B_m(T)$ is found to be strongly anisotropy dependent, however, in all cases the two lines always merge at the critical point [5,6]. This finding is a strong indication that the two lines represent one continuous vortex-lattice transition which is a first-order at high temperatures, but possibly becomes second-order at some sample-dependent T_{cp} as the temperature is decreased.

At fields above the B_{sp} line, significant bulk pinning is observed. Figure 4 shows the behavior of the apparent critical current in this region. It is important to note that in this region surface barriers also contribute significantly to the magnetic hysteresis. Therefore one cannot readily determine the critical current from the global magnetization measurements. In local measurements a proper analysis of the field gradient dB_z/dx can be made [4] which allows separation of the two contributions. Figure 4 thus represents the hysteretic behavior of the field gradient which reflects bulk pinning. The apparent critical current decreases rapidly with increasing temperature and

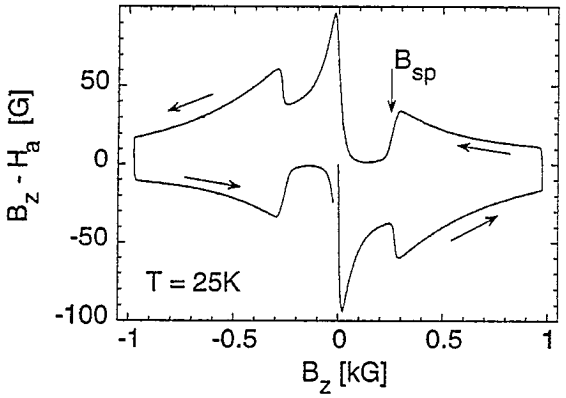

Figure 3: Local magnetization loop in the vicinity of the second magnetization peak B_{sp}.

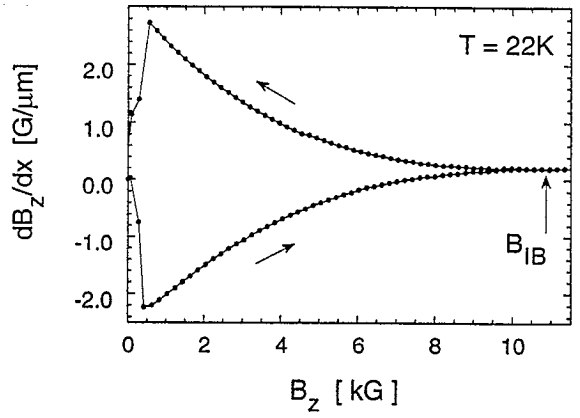

Figure 4: Field gradient dB_z/dx vs. the local induction B_z at low temperature. The locations of the corresponding sensors across the sample were chosen in order to reflect bulk pinning rather than surface barriers. B_{IB} thus indicates the position of the bulk irreversibility line.

field, and vanishes at $B_{IB}(T)$ [4]. We believe that this line in Fig. 1 approximately reflects the position of another phase boundary which extrapolates to the critical point T_{cp}.

4. COLUMNAR DEFECTS

In the as-grown BSCCO crystals the phase below $B_m(T)$ line in Fig. 1 is practically unpinned with effectively zero critical current, and therefore in principle could be either in a liquid or a solid phase. Hence there is a need for a direct test of the shear modulus in this phase. We have introduced a very low dose of columnar defects such that their density is much lower than the vortex density over a range of fields below $B_m(T)$ [7]. This case is similar to trying to tack a carpet with few nails. If the vortex matter is in a solid phase with a finite shear modulus the entire lattice will be pinned. On the other hand, in a liquid phase the unpinned vortices will flow freely around the few vortices trapped by the columns and the critical current will remain zero. Local dc magnetization measurements indicate that below $B_m(T)$ the shear modulus is indeed finite [7]. Here we present similar behavior measured by a local ac technique. Figure 5 shows the local ac response B'_{ac}/H_{ac} as a function of the applied dc field H_{dc} in the as-grown crystal along with a crystal irradiated to a dose corresponding to $B_\phi = 20$ G. In the as-grown sample the FOT manifests as a sharp paramagnetic peak which is the result of the thermodynamic step in the equilibrium magnetization at the transition [8]. Above B_m the sample exhibits no shielding, $B'_{ac}/H_{ac} = 1$, and the critical current is zero. The same is also true in the vicinity of the transition below B_m in as-grown samples, which means that in these samples the critical current is practically zero below the FOT. At lower fields, significant shielding is observed due to the presence of the geometrical barrier. This barrier also results in the unusual negative local response [9] as seen in Fig. 5 at $H_{dc} \simeq 20$ Oe. In the irradiated sample, however, the situation is dramatically different. Above B_m the sample is still unshielded, however full shielding is immediately established just below the transition, indicating a large critical current and the existence of a finite shear modulus in this phase which vanishes abruptly at the FOT. The same conclusions were recently reached on the basis of transport measurements [10,11]. It is interesting to note here that at elevated temperatures the FOT is still preserved in presence of low doses of columnar defects as demonstrated in Fig. 5 by the presence of the paramagnetic peak at the transition. The height of the peak

is somewhat suppressed relative to the unirradiated sample. At lower temperatures this peak is not detected. The small difference in the position of $B_m(T)$ for the two samples in Fig. 5 is due to some difference in the crystals and mainly in their sizes which results in different values of the internal field B at a given H_{dc}.

5. VORTEX MATTER PHASE DIAGRAM

Based on the above results we conclude that the phase below the FOT is a solid lattice which according to the neutron diffraction and μSR data has a long range orientational order [12]. We therefore refer to this state as a quasilattice [13]. At elevated temperatures the quasilattice melts through a FOT (see Fig. 1). Recent flux transformer measurements [11] indicate that this FOT is a sublimation transition in which the solid quasilattice transforms directly into a gas of pancake vortices. At lower temperatures the quasilattice transforms into a highly disordered entangled vortex solid through a disorder-driven transition at the second magnetization peak $B_{sp}(T)$ [13,14]. This disordered solid eventually melts continuously near the depinning line $B_{IB}(T)$.

Various parts of this work were supported by the German-Israeli Foundation - GIF, by the US - Israel Binational Science Foundation, by Minerva Foundation, Munich/Germany, by contract CT1*CT93-0063 from the Commission of the European Union, by the Dutch Foundation for Fundamental Research on Matter (FOM), and by the U.S. Department of Energy, BES-Material Sciences, under Contract No. W-31-109-ENG-38.

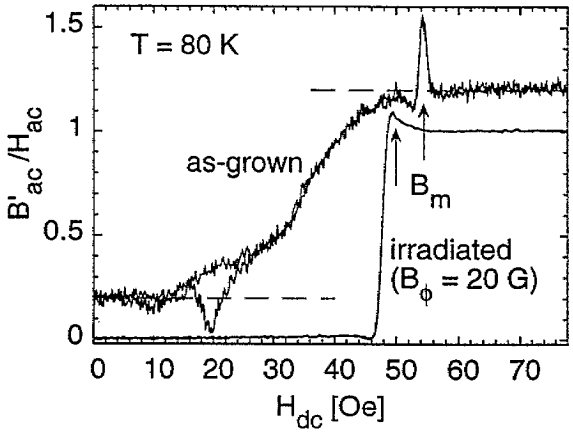

Figure 5: Normalized local ac response B'_{ac}/H_{ac} in the as-grown (shifted by 0.2 for clarity) and heavy-ion irradiated BSCCO crystals ($H_{ac} \approx 0.5$ G). The FOT is observed as a paramagnetic peak at $B_m(T)$ ($B'_{ac}/H_{ac} > 1$) in both samples. In irradiated crystal bulk pinning is present below the FOT and it vanishes sharply at the transition.

REFERENCES

1. N. Motohira *et al.*, J. Ceram. Soc. Jpn. Int. Ed. **97**, 994 (1989).
2. E. Zeldov *et al.*, Nature **375**, 373 (1995).
3. N. Chikumoto *et al.*, Phys. Rev. Lett. **69**, 1260 (1992); Physica C **185-189**, 2201 (1991); G. Yang *et al.*, Phys. Rev. B **48**, 4054 (1993); T. Tamegai *et al.*, Physica C **223**, 33 (1993); K. Kishio *et al.*, in "Proc. 7th Intnl. Workshop on Critical Currents in Superconductors" ed. H.W. Weber, World Sci. Pub., Singapore, p. 339 (1994).
4. E. Zeldov *et al.*, Europhys. Lett. **30**, 367 (1995); D. Majer *et al.*, Physica C 235-240, 2765 (1994).
5. B. Khaykovich *et al.*, Phys. Rev. Lett. **76**, 2555 (1996).
6. T. Hanaguri *et al.*, Physica C **256**, 111 (1996).
7. B. Khaykovich *et al.*, preprint.
8. N. Morozov *et al.*, Phys. Rev. B **54**, R3784 (1996); B. Schmidt *et al.*, Phys. Rev. B (in press).
9. N. Morozov *et al.*, Phys. Rev. Lett. **76**, 138 (1996).
10. H. Pastoriza and P.H. Kes, Phys. Rev. Lett. **75**, 3525 (1995); S. Watauchi *et al.*, Physica C **259**, 373 (1996); D. T. Fuchs *et al.*, Phys. Rev. B **54**, 796 (1996).
11. D. T. Fuchs *et al.*, Phys. Rev. B (in press).
12. R. Cubitt *et al.*, Nature **365**, 407 (1993); S. L. Lee *et al.*, Phys. Rev. Lett. **71**, 3862 (1993).
13. V. Vinokur *et al.*, preprint.
14. D. Ertas and D. R. Nelson, Physica C **272**, 79 (1996) and references therein.